



# Metabolic and proteomic mechanism of bisphenol A degradation by *Bacillus thuringiensis*

Chongshu Li<sup>a</sup>, Qiyong Lu<sup>b</sup>, Jinshao Ye<sup>a,\*</sup>, Huaming Qin<sup>a</sup>, Yan Long<sup>a</sup>, Lili Wang<sup>a</sup>, Huase Ou<sup>a</sup>

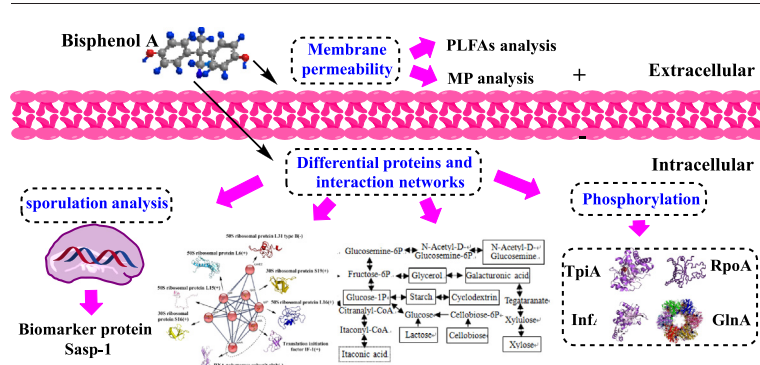
<sup>a</sup> School of Environment, Guangdong Key Laboratory of Environmental Pollution and Health, Jinan University, Guangzhou 510632, Guangdong, China

<sup>b</sup> College of Biology and Food Engineering, Guangdong University of Education, Guangzhou 510303, Guangdong, China

## HIGHLIGHTS

- Bisphenol A could be degraded effectively by *Bacillus thuringiensis*.
- BPA altered the expression of ribosomal proteins and phospholipids.
- BPA enhanced C14:0, C16:1 $\omega$ 7, C18:2 $\omega$ 6, C18:1 $\omega$ 9t and C18:0 synthesis.
- SasP-1 could be a biomarker to reflect impairment of spore DNA by BPA.
- BPA increased C18:1 $\omega$ 9t/C18:1 $\omega$ 9c and ratios of unsaturated/saturated PLFAs.

## GRAPHICAL ABSTRACT



## ARTICLE INFO

### Article history:

Received 4 February 2018

Received in revised form 10 May 2018

Accepted 28 May 2018

Available online 5 June 2018

Editor: Kevin V. Thomas

### Keywords:

Proteomics  
Degradation  
Phosphorylation  
Fatty acids  
iTRAQ

## ABSTRACT

Bisphenol A (BPA) is a worldwide, widespread pollutant with estrogen mimicking and hormone-like properties. To date, some target biomolecules associated with BPA toxicity have been confirmed. The limited information has not clarified the related metabolism at the pathway and network levels. To this end, metabolic and proteomic approaches were performed to reveal the synthesis of phospholipids and proteins and the metabolic network during the BPA degradation process. The results showed that the degradation efficiency of 1  $\mu\text{M}$  of BPA by 1  $\text{g L}^{-1}$  of *Bacillus thuringiensis* was up to 85% after 24 h. During this process, BPA significantly changed the membrane permeability; altered sporulation, amino acid and protein expression, and carbon, purine, pyrimidine and fatty acid metabolism; enhanced C14:0, C16:1 $\omega$ 7, C18:2 $\omega$ 6, C18:1 $\omega$ 9t and C18:0 synthesis; and increased the *trans/cis* ratio of C18:1 $\omega$ 9t/C18:1 $\omega$ 9c. It also depressed the spore DNA stability of *B. thuringiensis*. Among the 14 upregulated and 7 down-regulated proteins, SasP-1 could be a biomarker to reflect BPA-triggered spore DNA impairment. TpiA, RpoA, GlnA and InfA could be phosphorylated at the active sites of serine and tyrosine. The findings presented novel insights into the interaction among BPA stress, BPA degradation, phospholipid synthesis and protein expression at the network and phylogenetic levels.

© 2018 Elsevier B.V. All rights reserved.

## 1. Introduction

Bisphenol A (BPA) is an organic synthetic compound belonging to the group of diphenylmethane derivatives and bisphenols. It exhibits estrogen mimicking and hormone-like properties and causes carcinogenicity (Haighton et al., 2002), reproductive toxicity (Maffini et al., 2006),

\* Corresponding author.

E-mail address: [jsye@jnu.edu.cn](mailto:jsye@jnu.edu.cn) (J. Ye).

immunotoxicity (Yin et al., 2007), embryotoxicity (Zhou et al., 2011) and transgenerational influence (Berger et al., 2016; Dong et al., 2018) to various species. Its worldwide use in the production of synthetic polymers, including epoxy resins and polycarbonates (Flint et al., 2012), has triggered contamination in packing materials and ecosystems.

At the bimolecular level, some genes associated with the immune system in human osteosarcoma cells (Fic et al., 2015) and genes regulated by miRNAs (Cho et al., 2010) in the Sertoli cell line of mice have been found to be related to BPA resistance. The presence of these target genes is unnecessary meaning their transcription and translation. Therefore, proteins with a vast array of functions, including metabolic reaction catalysis, DNA replication, stimuli response and molecular transport, became a critical group of target biomolecules. Previous studies have confirmed that BPA triggered the alteration of retinoblastoma-associated protein, increased the production of Rho GTPases and cell division cycle protein CDC42 (Williams et al., 2016), and stimulated the expression of prostaglandin D2 synthase in adult rats (Wu et al., 2015) as well as dysregulated sera proteins in rat serum (Betancourt et al., 2014). The proteins apo-AI, DPPIII and VAT were selected as biomarkers in prenatal mouse immune organs (Yang et al., 2008) to reflect BPA toxicity.

BPA resistance, transport and transformation are associated with cellular regulatory, signaling and metabolic networks. The limited information available on only some individual biomolecules is not enough to reveal the networks related to BPA degradation. Proteomic technology is an insightful tool to clarify these types of mechanisms. For example, two-dimensional gel electrophoresis has been used to investigate a target enzyme (hydroquinone dioxygenase) for BPA resistance expressed in *Sphingomonas* TTNP3 (Collado et al., 2013). Quantitative label-free technology has also been applied to reveal (Zhou et al., 2015) the differential expression of proteins possibly associated with BPA transformation. To date, these investigations didn't reveal the mechanisms of the metabolic networks and protein interactions related to BPA degradation.

Phospholipid fatty acids (PLFAs) are another important class of biomolecules that can be used as biomarkers of responses to stress (Arisawa et al., 2016). For example, the *trans/cis* ratio of PLFAs and that of unsaturated PLFAs/saturated PLFAs has been used to reflect cell stability under xenobiotic exposure. In particular, some types of PLFAs could be split to generate products that function as second messengers in signal transduction. For example, (4, 5)-bisphosphate phosphatidylinositol could be catalyzed by phospholipase C into triphosphate inositol and diacylglycerol, which initiate the release of calcium ions and the activation of protein kinase C (Choi et al., 2005; Penniston et al., 2014). Given that both PLFAs and the proteome have the essential molecular and metabolic functions, their synergetic synthesis will be the critical scientific objective to clarify the mechanism related to pollutant degradation. Therefore, the current study will provide insight into the relationship among BPA degradation, PLFA synthesis, protein expression and the metabolic network.

*Bacillus thuringiensis* is a Gram-positive bacterium that produces insecticidal proteins which are widely used as biopesticides in insect control (Bravo et al., 2017). As an important model microbe, *B. thuringiensis* contains enzymes that cleave benzene ring-containing pollutants, including dimethyl phthalate (Brar et al., 2009), fipronil (Mandal et al., 2013) and triphenyltin (Wang et al., 2017). Therefore, it was used in the current study to degrade BPA. The metabolic and proteomic responses of cells were analyzed. The potential findings can present new insights into BPA degradation by microbes at the proteomic level and the metabolic network.

## 2. Materials and method

### 2.1. Strain and chemicals

*B. thuringiensis* GIMCC1.817 was an effective strain for the degradation of multiple pollutants (Tang et al., 2016) and was stored at the Microbiology Culture Center of Guangdong Province, China. BPA was purchased from Sigma Aldrich (St. Louis, MO, USA) and was dissolved

in chromatography-grade methanol. Trypsin (Promega, V5280, USA) and an iTRAQ reagent multiplex kit (Sigma, PN 4352135, USA) were used in this experiment.

### 2.2. Microbial culture and bisphenol A degradation

*B. thuringiensis* was inoculated into a nutrient medium containing (in g L<sup>-1</sup>) 5 NaCl, 10 peptone and 3 beef extract at 30 °C in a rotary shaker at 120 r min<sup>-1</sup> for 24 h. Cells were separated from the medium by centrifugation at 6000 r min<sup>-1</sup> for 5 min and then washed three times with sterile water. The treatment medium used for BPA degradation included (in g L<sup>-1</sup>) 0.03 KH<sub>2</sub>PO<sub>4</sub>, 0.07 NaCl, 0.03 NH<sub>4</sub>Cl, 0.01 MgSO<sub>4</sub>, 0.03 beef extract and 0.1 peptone. For BPA degradation, 20 mL treatment medium containing 1 μM of BPA and 1 g L<sup>-1</sup> of cells was inoculated into a 50 mL Erlenmeyer flask in the dark at 30 °C on a rotary shaker at 120 r min<sup>-1</sup> for 24 h. A control treatment without cells was also performed. There were three biological replicates for each sample. The treatment and control samples were extracted by ultrasound-assisted liquid-liquid extraction with 20 mL dichloromethane, concentrated to 0.5 mL and solvent-exchanged into 4 mL methanol, then analyzed by high-performance liquid chromatography with a tandem mass spectrometer (Applied Biosystems SCIEX 5500, USA). Quality assurance and quality control included using a laboratory solvent blank, a matrix blank, a matrix spike and a matrix spike duplicate. The recovery of BPA in the spiked treatment media was 96 ± 2%. The intermediates of BPA degradation were detected using a time-of-flight HRMS (TripleTOF 5600, Applied Biosystems SCIEX, USA).

### 2.3. Carbon substrate metabolism for bisphenol A degradation

Biolog microplates were used to analyze cellular activities of carbon nutrient metabolism before and after BPA degradation. The plates contained 96 wells with 31 kinds of carbon nutrients. Briefly, cells after BPA degradation were diluted 100 times in 0.85% sterilized saline solution, followed by inoculation of 150 μL of the mixture into each well of the microplates at 25 °C in the dark. The optical density at 590 nm of each well was determined every 24 h. The network related to carbon metabolism for BPA degradation was mapped through the KEGG database (<http://www.kegg.jp/>).

### 2.4. Protein preparation

After BPA treatment for 24 h, cells before and after degradation were suspended in 1 mL lysis buffer (15 mM Tris-HCl, 7 M urea, 2 M thiourea, 1% w/v dithiothreitol, 4% w/v 3-[(3-cholamidopropyl)dimethylammonio]propanesulfonate with 0.2 g L<sup>-1</sup> phenylmethylsulfonyl fluoride, 2% v/v IPG buffer and 0.6 g L<sup>-1</sup> dithiothreitol). After vibration for 10 s, the samples were frozen thrice in liquid nitrogen for 15 min each time, followed by ultrasonication for 20 min. Subsequently, a nuclease mix was added to the lysate at a final concentration of 1% v/v. After the mixture was incubated at 4 °C for 30 min, the cell debris was removed at 4 °C by centrifugation at 12000 r min<sup>-1</sup> for 1 h. The concentration of protein was measured using the Bradford method.

### 2.5. Protein digestion

Proteins from each sample were reduced with 2 μL reducing reagent in a water bath at 37 °C for 1 h. The cysteines in proteins were blocked with 1 μL cystein-blocking reagent for 10 min at 25 °C. After adding to 10 kDa Amicon Ultra-0.5 centrifugal filter devices, the protein samples were separated at 12000 r min<sup>-1</sup> for 20 min and washed three times with 100 μL dissolution buffer each time. The samples in the filter devices were digested by 50 μL trypsin at 4% w/w 12 h at 37 °C. Subsequently, the samples were centrifuged at 12000 r min<sup>-1</sup> for 20 min and digested by 1 μg trypsin for 2 h. After centrifugation, the liquid in

the collection tube was collected. The concentration of tryptic peptides was measured using the Bradford method.

## 2.6. iTRAQ labeling and desalination

Tryptic peptides were labeled with an iTRAQ reagent multiplex kit according to the manufacturer's instructions. Briefly, after protein digestion by trypsin, the peptides of the control sample without BPA and of the experimental group were labeled with tag 114 and 115. Ethanol at 150  $\mu\text{L}$  was added to each tube of iTRAQ reagent, followed by vortexing and spinning. After the tryptic peptides were transferred to a new tube, 100  $\mu\text{L}$  chromatographic-grade water was added to each sample to stop the reaction. One microliter of solution from each sample was detected by ABI 4800 MALDI TOF/TOF (Applied Biosystems, Foster City, CA) to determine the labeling efficiency. Subsequently, the iTRAQ-labeled samples were mixed, vortexed, spun, desalinated with Strata-X (Phenomenex, USA), and separated by strong cation exchange chromatography. The labeled peptides were dried in a vacuum concentrator. The samples were then resolved with solution (2% v/v acetonitrile, 0.1% v/v formic acid), centrifuged at 12000  $\text{r min}^{-1}$  for 20 min, and detected by an AB Sciex Triple-TOF 5600 mass spectrometer (AB Sciex, Framingham, MA, USA) equipped with a Nanospray III source (AB Sciex).

## 2.7. Protein identification and bioinformatics analysis

Protein identification in the UniProt Database and relative iTRAQ quantification were performed with ProteinPilot™ Software 4.5 (AB SCIEX). For iTRAQ quantification, peptides were automatically selected by the Pro Group™ algorithm to calculate the reporter peak area, error factor and *p* value. A reverse database search strategy was adopted to estimate the fault occurrence rate for peptide identification. A strict unused confidence score of higher than 1.3, which corresponded to at least a peptide confidence level of 95%, was used as the qualification criterion. Identified proteins with at least two matched peptides at higher than 95% confidence and an FDR value lower than 1% were used to perform protein quantification. Subsequently, proteins with at least a 1.2-fold increase or decrease were identified as the differentially expressed proteins. The PANTHER Database (<http://www.pantherdb.org/>) was used to classify the proteins. The functions, interactions and phosphorylation sites of these differential proteins were annotated through the PANTHER Classification System (<http://www.pantherdb.org/>), DAVID Bioinformatics Resources 6.7 (<https://david.ncifcrf.gov>), STRING 10 (<http://string-db.org>) and dbPSP Database (<http://dbpsp.biocuckoo.org>), respectively.

## 2.8. PLFAs extraction and membrane potential assay

PLFAs extraction and methylation and membrane potential analysis were conducted according to a previous study (Wang et al., 2017). PLFAs were detected and analyzed by gas chromatography–mass spectrometry (Shimadzu, Japan). The membrane potential was measured by a FACS Aria flow cytometer (BD, USA), with 10,000 cells being acquired per sample at a flow rate of 10  $\text{mL min}^{-1}$ . Fluorescent dye JC-1 (5,5',6,6'-tetrachloro-1,1',3,3'-tetraethylbenzimidazolcarbocyanineiodide) was used to dye the cells. The high and low electric potentials formed red fluorescence aggregates and green fluorescence monomers, respectively. Differences in means of the data of PLFAs and membrane potential were analyzed by one-way ANOVA with Duncan's test.

## 3. Results and discussion

### 3.1. Bisphenol A degradation and carbon substrate metabolism

The degradation efficiency of BPA at 1  $\mu\text{M}$  in the treatment solution by comparison with the control was 85% (Table S1). Its potential intermediate 2,2-bis(4-hydroxyphenyl)-1-propanol ( $\text{C}_{15}\text{H}_{16}\text{O}_3$ , MW = 244) was identified by LC-MS-MS (Table S2). This finding and previous reports related to BPA degradation by NADPH (Fischer et al., 2010a), NADH and cytochrome P450 (Sasaki et al., 2005) inferred that BPA was initially transformed to 2,2-bis(4-hydroxyphenyl)-1-propanol in pathway I, then to 4-hydroxyphenol and 4-(2-propanol)-phenol in pathway II by *B. thuringiensis*, followed by the generation of 2,3-bis(4-hydroxyphenyl)-1,2-propanediol, 4-hydroxyphenacyl alcohol and 4-hydroxybenzoate. The proposed degradation pathway of BPA is shown in Fig. 1 A. This pathway shows the potential mineralized and degraded process of BPA by *B. thuringiensis*.

To reveal the relationship between carbon metabolism and BPA degradation for the regulation of BPA biotransformation, the cellular metabolism of 31 kinds of carbon substrates was examined. With time extension, the enhanced degradation of 2-hydroxybenzoate, 4-hydroxybenzoate, phenylalanine and phenylethylamine clarified that *B. thuringiensis* could utilize benzene ring compounds as sole carbon nutrients (Fig. 1 B and C). It is direct evidence to prove why this species could degrade BPA effectively. The degradation of BPA did not trigger a significant difference in the utilization of these compounds. This finding infers that the expression of enzymes for BPA degradation did not upregulate the transformation of compounds with similar structures.

The metabolism of D-galactonic acid-lactone, pyruvate methyl ester, xylose, galacturonic acid, L-asparagine, Tween 40, Tween 80, serine,  $\alpha$ -cyclodextrin, N-acetyl-D-glucosamine, r-hydroxybutyric acid, cellobiose, glucose-1-phosphate, ketobutyric acid, lactose, glycerol and putrescine after BPA degradation was upregulated, whereas that of glucosaminic acid and itaconic acid was down-regulated.

In the upregulated metabolic pathways, starch and sucrose metabolic transformation of polysaccharides into monosaccharide, glycolysis conversion of glucose into pyruvate, pyruvate oxidation to generate acetyl-CoA, fatty acid metabolism connected via acetyl-CoA and glycerol, and amino acid metabolism were also activated by BPA degradation (Fig. 1D). This finding confirms that the majority of central metabolic pathways were upregulated by the degradation of BPA, while the toxicity of BPA at the studied concentration and its intermediates did not trigger significant inhibitive effects on cellular metabolic pathways due to the rapid degradation of those compounds.

Extracellular glucosaminic acid needs to be phosphorylated through catalysis by DgaA during the transportation process. Glucosaminic acid-6-phosphate ammonia lyase catalyzes a reaction converting glucosaminic acid-6-phosphate to ammonia and 2-dehydro-3-deoxy-6-phospho-D-gluconate. This product is further transformed to 3-phosphoglycerate and degraded in the glycolysis pathway. Based on the fact that glycolysis is upregulated after BPA degradation, it can be deduced that the cleavage of the carbon nitrogen bond for ammonia removal is the limiting step for the down-regulation of glucosaminic acid metabolism in the current study. This finding confirmed that BPA degradation inhibited the activity of ammonia lyase. Another down-metabolized substrate, itaconic acid, is successively catalyzed by succinyl-CoA synthetase, itaconyl-CoA hydratase and citramalyl-CoA lyase during the formation of pyruvate. This process was inhibited by the degradation of BPA.

**Fig. 1.** The proposed degradation pathway of bisphenol A by *B. thuringiensis* and carbon substrate metabolism for the degradation of bisphenol A. (A) Proposed degradation pathway of bisphenol A by *Bacillus thuringiensis* (a: 2,2-bis(4-hydroxyphenyl)-1-propanol was identified in this study; b: CoA is coenzyme A; c: Reactions obtained from the KEGG database. Dotted arrows indicate reactions omitted by the KEGG database). (B) Metabolism of the control cells before bisphenol A degradation. (C) Metabolism of the samples after degradation of 1  $\mu\text{M}$  of BPA by 1  $\text{g L}^{-1}$  of cells for 24 h. (D) Metabolic networks regulated by bisphenol A degradation. Compounds in solid rectangles were upregulated, whereas those in dashed rectangles were down-regulated.



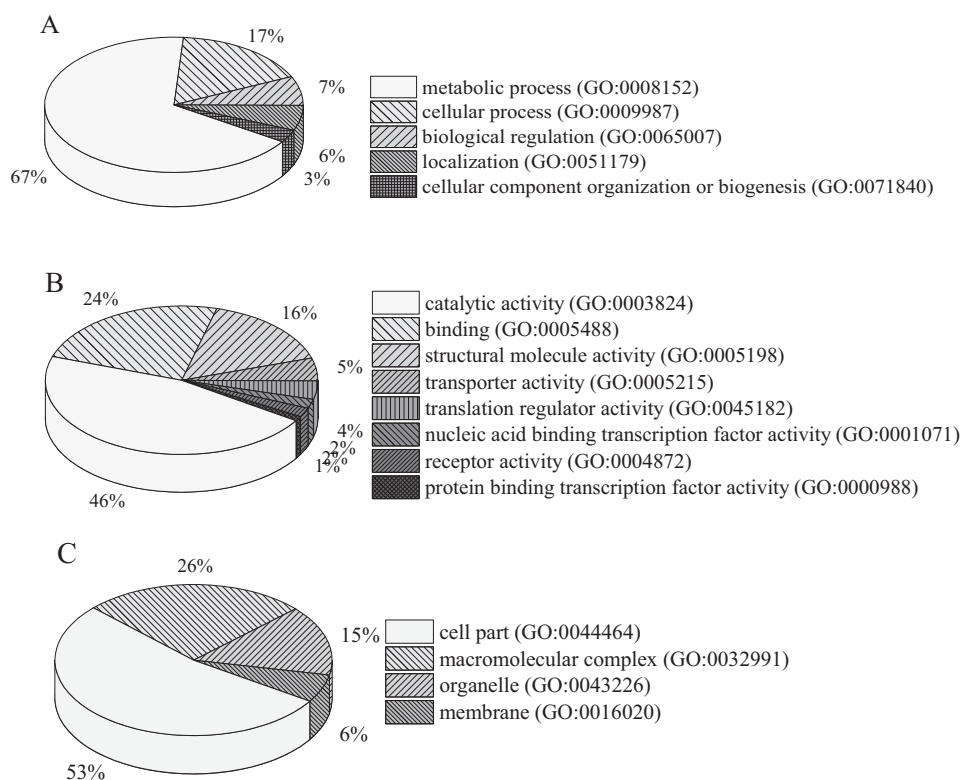


**Fig. 2.** The percentage of 125 proteins in biological processes (A), molecular functions (B) and cellular component (C), respectively.

### 3.2. Proteins clusters and interaction networks

Among the 125 quantifiable identified proteins (Table S3), 14 and 7 of them were up and down-regulated (Table S4 and S5), respectively, after cells were exposed to BPA. Cellular component organization, or biogenesis, and localization of biological processes (Fig. 2A) accounted for 67% and 17% of the related functions, respectively. Regarding molecular functions (Fig. 2B), the proteins related to catalytic activity and binding and structural molecular activity were 46%, 24% and 16%, respectively. These proteins mainly came from the cell part (53%) and macromolecular complex (26%) of cellular component (Fig. 2C). The clustering coefficient of the differentially expressed proteins and the protein-protein interaction enrichment  $p$ -value were 0.741 and  $3.94e^{-11}$ , respectively, confirming that these proteins were significantly enriched in the dysregulated expression network. Fig. 3A exhibits that the upregulated proteins (RplF, RpsS, RplP, RplO, RpsP and InfA) and down-regulated proteins (Tkt, RpoA and RpmE2) existed in direct interaction.

The upregulated ribosomal proteins RplF, RpsS, RplP, RplO and RpsP implied that the polypeptide chain of the protein underwent increasing synthesis during the process of BPA degradation. TpiA and other associated proteins participated in 5 pathways (Fig. 3B). In these pathways, TpiA and YtsJ were overexpressed in gluconeogenesis, which is consistent with the upregulated metabolism of xylose,  $\alpha$ -cyclodextrin, cellobiose, glucose 1-phosphate and lactose (Fig. 1). The participation of the key node proteins TpiA, Tkt and GlnA in multiple metabolic pathways (Fig. 3B) demonstrated that BPA enhanced these metabolisms, which is consistent with Fig. 1. The overexpressed GlnA involved in the two-component system suggested increased nitrogen assimilation, which further enhanced glutamate metabolism (Fig. S1).

### 3.3. Differentially expressed ribosomal proteins and ribonuclease

The upregulation of RpsP, RpsS, RplO, RplP, and RplF and the down-regulation of RpmE2 clarified the differential translation of functional

genes regulating the expression of diverse proteins after BPA degradation (Fig. 4). The down-regulation of RpmE2 and DNA-directed RNA polymerase subunit alpha (RpoA) and the upregulation of translation initiation factor IF-1 (InfA) suggested that the translation process was differentially regulated for BPA degradation.

Ribonuclease is a ribonucleic acid (RNA) hydrolase which contributes to RNA metabolism and homeostasis. During the starvation period, the ribonuclease RNase PH utilizes phosphate to accumulate rRNA fragments and degrades the total RNAs (Basturea et al., 2011). Thus, its up-regulation is consistent with nutrient metabolism with time extension. Exoribonuclease RNase R is involved in mRNA degradation (Basturea et al., 2011), playing an important role in the quality control of ribosomes for precise translation (Domingues et al., 2015). Its down-regulation in the presence of BPA illustrated that BPA affected the translation process (Liang and Deutscher, 2013).

Synergy was found between cross-regulation and cotranscription of RNase R and SmpB (Moreira et al., 2012). The binding of RNA-SmpB stabilized the association of the protease subunit HslUV with the N-terminal region of RNase R (Liang and Deutscher, 2012), resulting in increased degradation of unfolded proteins generated due to down-regulation of the foldase protein PrsA1. In addition, overexpressed RNA-binding protein (Hfq) regulated mRNA translation in response to environmental stresses and modulated metabolite concentration by binding small regulatory RNA and mRNA. These findings inferred that BPA posed a risk to protein folding and translation.

### 3.4. Cellular homeostasis analysis with disulfide linkage formation and sporulation

Thiol-disulfide oxidoreductase (BdbD) is a key factor in determining protein folding and function (Feng and Coulombe, 2015). Its formation not only mediates the translocation and oxidation of mitochondrial transporters (Ramesh et al., 2016) but also promotes enzyme activity and stability (Lu et al., 2014). Its down-regulation during the process of BPA degradation revealed that BPA certainly influenced the enzyme

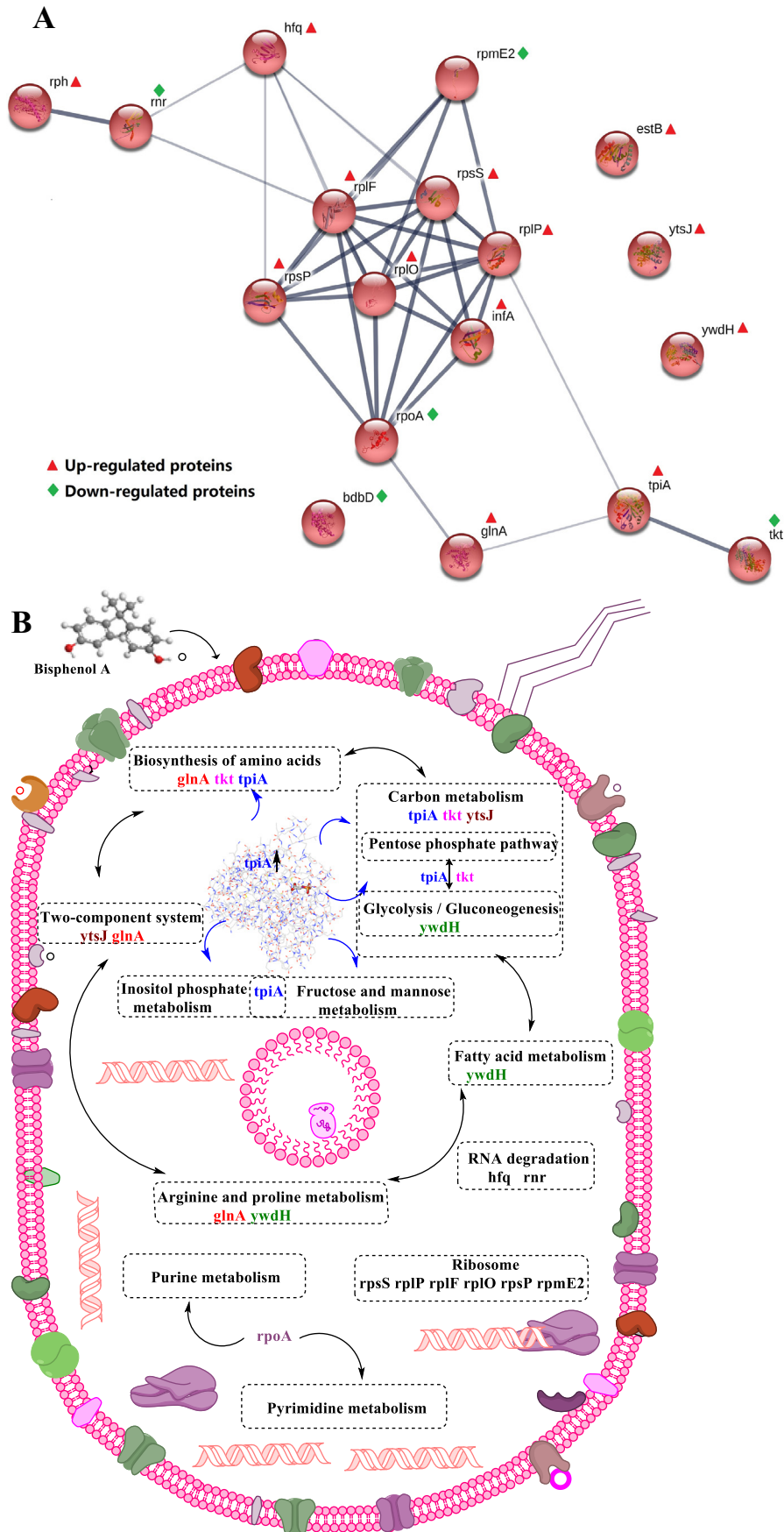


**Fig. 3.** (A) The interaction network of the identified differentially expressed proteins in *B. thuringiensis* after bisphenol A exposure. The thickness of the lines represents the connection degree. (B) The cellular metabolic pathways associated with differentially expressed proteins under exposure to bisphenol A.

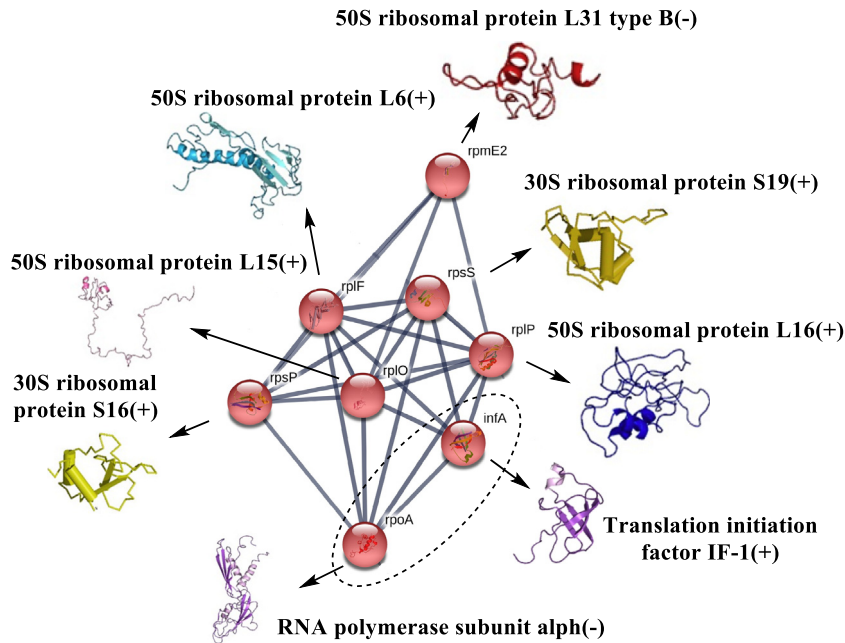


Fig. 4. Differential ribosomal proteins in the KEGG ribosome pathway. A plus sign stands for upregulation, and a minus sign indicates down-regulation.

activity, cellular biological process and cellular components (Fig. 2). Correspondingly, it coincided with the upregulated HsIV involved in unfolded protein degradation and the down-regulated foldase protein PrsA 1 associated with protein folding in the presence of BPA. Moreover, DsbA is an enzyme containing a thioredoxin domain (Erlendsson and Hederstedt, 2002) which is helpful in protein oxidative folding and is associated with bacterial spreading in natural environments (Crow et al., 2009). Its amino acid sequence shared 74 similar positions with BdbD, which revealed that they were orthologous proteins (Fig. 5A). This

finding further confirmed the biological function of BdbD. The above-mentioned functions revealed that BdbD played an important role in regulating the cellular homeostatic process under the stress of BPA.

Sporulation is also one of the signals that reflect cellular homeostasis under environmental stimuli. As an endospore-forming species, *B. thuringiensis* forms spores and minimizes cellular metabolism to resist nutrient limitation (Esfahani et al., 2016), ensuring cellular survival and evolution under adverse conditions (Tocheva et al., 2016). SasP are alpha/beta-type small, acid-soluble spore proteins

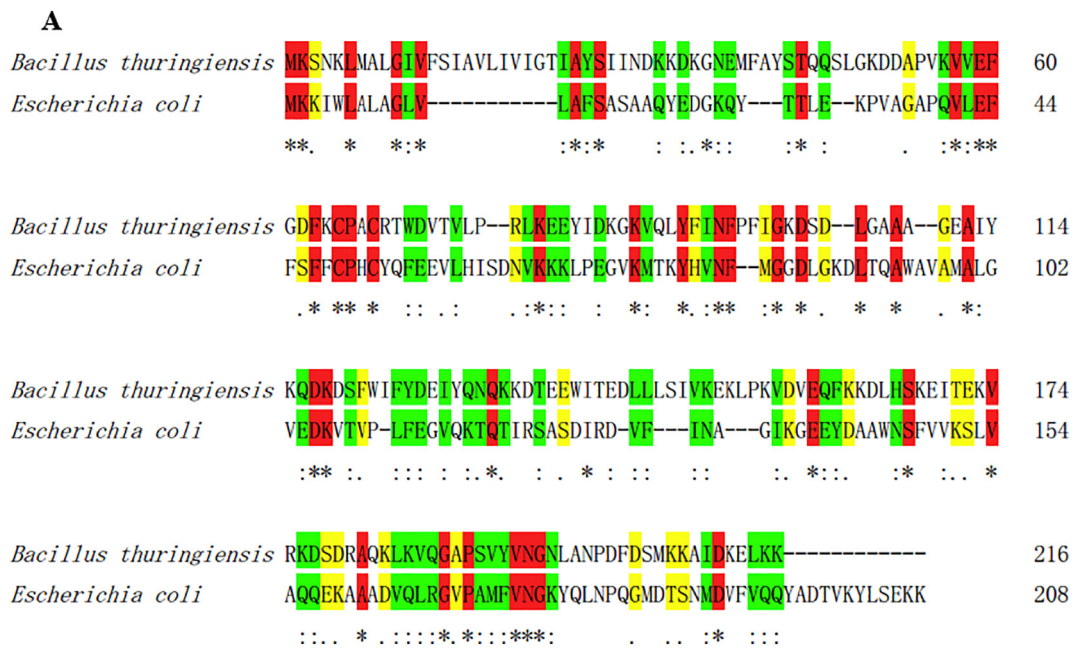


Fig. 5. (A) The sequence alignment of DsbA (*Escherichia coli*) and BdbD (*Bacillus thuringiensis*) by the CLUSTAL OMEGA (1.2.4). An asterisk (\*) indicates positions which have a single, fully conserved residue. A colon (:) indicates conservation between groups of strongly similar properties, scoring >0.5 in the Gonnet PAM 250 matrix. A period (.) indicates conservation between groups of weakly similar properties, scoring ≤0.5 in the Gonnet PAM 250 matrix, (B) The phylogeny tree (neighbor-joining) of 84 homologous strains of *B. thuringiensis* from the IMG database. (C) The phylogeny tree (neighbor-joining) of 42 orthologous strains of *B. thuringiensis* based on the SasP-1 sequence identified through BLAST.

B

*Bacillus thuringiensis*\_YC-10\_null\_replaces\_98239 : Ga0111320\_109  
*Bacillus thuringiensis*\_GOE3 (BtGoe3) : BTGOE3\_contig000013  
*Bacillus thuringiensis*\_Sbt003 : Ga0078284\_1010  
*Bacillus thuringiensis*\_sv\_kurstaki\_YBT-1520 : CP004858  
*Bacillus thuringiensis*\_BMB3201 : Ga0100705\_1054  
*Bacillus thuringiensis*\_AK47 : Ga0104883\_150  
*Bacillus thuringiensis*\_sv\_kurstaki\_HD-1 : CP004870  
*Bacillus thuringiensis*\_sv\_aizawai\_Leapi01 : AMXS02000112  
*Bacillus thuringiensis*\_sv\_kurstaki\_HD73 : CP004069  
*Bacillus thuringiensis*\_Bt185 : Ga0125079\_18  
*Bacillus thuringiensis*\_serovar\_Kurstaki\_HD\_1 : Ga0078034\_111  
*Bacillus thuringiensis*\_GOE4 (BtGoe4) : BTGOE4\_contig000013  
*Bacillus thuringiensis*\_GOE2 (BtGoe2) : BTGOE2\_contig000012  
*Bacillus thuringiensis*\_DB27 : Ga0056873\_1074  
*Bacillus thuringiensis*\_sv\_aizawai\_Hu4-2 : AMXT02000126  
*Bacillus thuringiensis*\_sv\_coreanensis\_ST7 : Ga0175594\_13  
*Bacillus thuringiensis*\_sv\_tolworthi\_tolworthi\_1 : Ga0133303\_11  
*Bacillus thuringiensis*\_823\_BTHU : Ga0104879\_154  
*Bacillus thuringiensis*\_YC-10 : Ga0098239\_11  
*Bacillus thuringiensis*\_serovar\_galleriae\_4G5 : Ga0077939\_109  
*Bacillus thuringiensis*\_serovar\_mexicanensis\_strain:27 : Ga0077500\_1013  
*Bacillus thuringiensis*\_sv\_kurstaki\_HD-1 : Ga0055125\_1120  
*Bacillus thuringiensis*\_KNU-07 : Chromosome  
*Bacillus thuringiensis*\_Bc601 : Ga0133451\_15  
*Bacillus thuringiensis*\_NBIN-866 : Ga0056801\_1015  
*Bacillus thuringiensis*\_sv\_kurstaki\_YBT-1520 : Ga0059241\_gi676317577.5  
*Bacillus thuringiensis*\_GOE1 (BtGoe1) : BTGOE1\_contig000011  
*Bacillus thuringiensis*\_YWC2-8 : Ga0123586\_13  
*Bacillus thuringiensis*\_sv\_Indiana\_HD521\_null\_replaces\_81812 : Ga0111351\_12  
*Bacillus thuringiensis*\_sv\_Indiana\_HD521 : Ga0081812\_11  
*Bacillus thuringiensis*\_sv\_Morrisoni\_HD\_600 : Ga0077611\_18  
*Bacillus thuringiensis*\_DAR\_81934 : Ga0060226\_116  
*Bacillus thuringiensis*\_serovar\_morrisoni\_BGSC\_4AA1 : Ga0077848\_11  
*Bacillus thuringiensis*\_sv\_alesti\_BGSC\_4C1 : Ga0133529\_14  
*Bacillus thuringiensis*\_NRRL\_B-18247\_re-assembly\_(BTD) : BTI247\_contig000001  
*Bacillus thuringiensis*\_HD12 : Ga0125139\_15  
*Bacillus thuringiensis*\_HD-771 : CP003752  
*Bacillus thuringiensis*\_DAR\_81934 : D828DRAFT\_ANPK01000015\_1.15  
*Bacillus thuringiensis*\_sv\_israelensis : JEOC01000012  
*Bacillus thuringiensis*\_HD1002 : Ga0077856\_18  
*Bacillus thuringiensis*\_Lr7/2 : Ga0069197\_125  
*Bacillus thuringiensis*\_HD-789 : CP003763  
*Bacillus thuringiensis*\_MYBT18246 : Ga0174755\_105  
*Bacillus thuringiensis*\_BR58 : Ga0124690\_1054  
*Bacillus thuringiensis*\_147 : Ga0098729\_187  
*Bacillus thuringiensis*\_sv\_israelensis\_(re-annotation\_Oct\_2015) : Ga0097831\_1185  
*Bacillus thuringiensis*\_NRRL\_B-18246\_(BTC) : BT246\_contig000001  
*Bacillus thuringiensis*\_T01-328 : ARXZ02000011  
*Bacillus thuringiensis*\_YBT-1518 : CP005935  
*Bacillus thuringiensis*\_sv\_tolworthi\_NA205-2 : J098DRAFT\_AYXQ01000112\_1.112  
*Bacillus thuringiensis*\_sv\_thuringiensis\_IS5056 : CP004123  
*Bacillus thuringiensis*\_Bt407 : CP003889  
*Bacillus thuringiensis*\_GOE07 (BtGoe7) : BTGOE7\_contig000002  
*Bacillus thuringiensis*\_GOE5 (BtGoe5) : BTGOE5\_contig000001  
*Bacillus thuringiensis*\_CTC : Ga0125289\_12  
*Bacillus thuringiensis*\_LMI212 : LM1212DRAFT\_AYPV01000009\_1.9  
*Bacillus thuringiensis*\_Lr3/2 : Ga0069193\_139  
*Bacillus thuringiensis*\_97-27\_null\_replaces\_81718 : Ga0111280\_11  
*Bacillus thuringiensis*\_HD682 : Ga0100887\_11  
*Bacillus thuringiensis*\_HD571 : Ga0100911\_11  
*Bacillus thuringiensis*\_Et10/1 : Ga0069194\_1432  
*Bacillus thuringiensis*\_HD1011 : Ga0100879\_11  
*Bacillus thuringiensis*\_HD571\_null\_replaces\_100911 : Ga0111338\_11  
*Bacillus thuringiensis*\_HD682\_null\_replaces\_100887 : Ga0111359\_12  
*Bacillus thuringiensis*\_97-27 : Ga0081718\_11  
*Bacillus thuringiensis*\_HS18-1\_null\_replaces\_98193 : Ga0111325\_102  
*Bacillus thuringiensis*\_HS18-1 : Ga0098193\_11  
*Bacillus thuringiensis*\_GOE06 (BtGoe6) : BTGOE6\_contig000001  
*Bacillus thuringiensis*\_ZBG4 : Ga0104918\_1026  
*Bacillus thuringiensis*\_MC28 : CP003687  
*Bacillus thuringiensis*\_serovar\_thuringiensis\_str\_T01001\_unfinished\_sequence : NZ\_ACNA01000002  
*Bacillus thuringiensis*\_serovar\_tochigiensis\_BGSC\_4YI\_unfinished\_sequence : NZ\_ACMY01000002  
*Bacillus thuringiensis*\_serovar\_pondicheriensis\_BGSC\_4BA1\_unfinished\_sequence : NZ\_ACNH01000003  
*Bacillus thuringiensis*\_serovar\_monterrey\_BGSC\_4AJ1\_unfinished\_sequence : NZ\_ACNE01000003  
*Bacillus thuringiensis*\_serovar\_pulsiensis\_BGSC\_4CCI\_unfinished\_sequence : NZ\_ACNJ01000003  
*Bacillus thuringiensis*\_serovar\_andalusiensis\_BGSC\_4AW1\_unfinished\_sequence : NZ\_ACNG01000005  
*Bacillus thuringiensis*\_serovar\_pakistani\_str\_T13001\_unfinished\_sequence : NZ\_ACNC01000002  
*Bacillus thuringiensis*\_IBL\_4222\_unfinished\_sequence : NZ\_ACNL01000002  
*Bacillus thuringiensis*\_IBL\_200\_unfinished\_sequence : NZ\_ACNK01000002  
*Bacillus thuringiensis*\_serovar\_sotto\_str\_T04001\_unfinished\_sequence : NZ\_ACNB01000002  
*Bacillus thuringiensis*\_serovar\_kurstaki\_str\_T03a001\_unfinished\_sequence : NZ\_ACND01000002  
*Bacillus thuringiensis*\_serovar\_huazhongensis\_BGSC\_4BD1\_unfinished\_sequence : NZ\_ACNI01000002

0.10

Fig. 5 (continued).

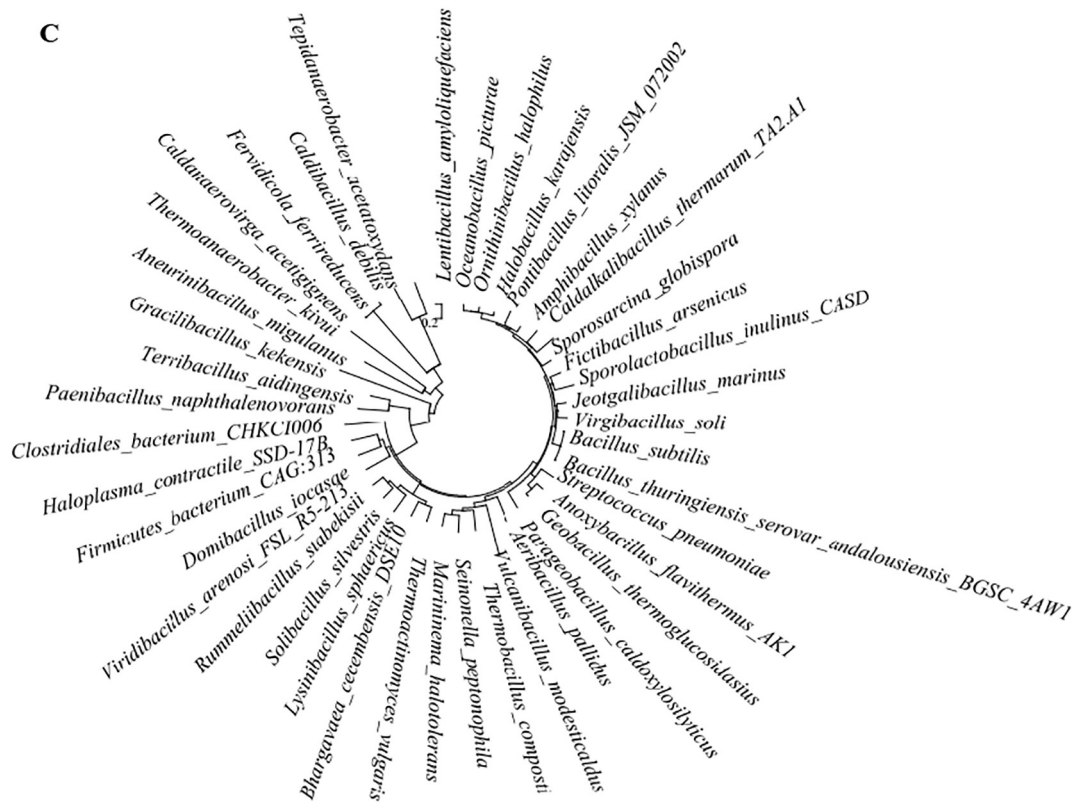


Fig. 5 (continued).

that nonspecifically bind to DNA in spores of *Bacillus* species. They can protect the bound DNA backbone from chemical and enzymatic cleavage by reducing the rate of DNA depurination (Setlow et al., 2006) and are, thus, involved in the high resistance of spores to various stresses. The down-regulation of SasP-1 (major beta-type SasP) during the process of BPA degradation in the current study meant that BPA could pose some cleavage risk to the spore DNA. Therefore, SasP-1 can be a potential biomarker to reflect pollutant stress to the stability of spore DNA.

To verify the above inference and determine whether SasP-1 contains a stable domain or sequence in different species of *Bacillus*, the homology of SasP-1 expressed in different strains and species was calculated. Ninety homologous strains of *B. thuringiensis* were found in the IMG database (<https://img.jgi.doe.gov>). Eighty-two of them (Fig. 5B) contained the functional gene that expressed this protein. Based on sequence similarity, 42 orthologous proteins of SasP-1 were found (Fig. 5C). The presence of this protein in these strains with endospores further confirmed that it could be a biomarker to reflect pollutant stress.

### 3.5. Relationship between protein phosphorylation and BPA degradation

To date, the limited evidence related to phosphorylation of functional proteins did not clarify the relation between protein phosphorylation and pollutant recognition, transport, resistance and transformation. In the current study, the serine and threonine phosphorylation sites (Table S6) of differentially expressed proteins were predicted using NetPhosBac 1.0 Server (<http://www.cbs.dtu.dk/services/NetPhosBac/>). These phosphorylation proteins were verified by dbPSP (<http://dbpsp.biocuckoo.org/> (Pan et al., 2015)). Different phosphorylation sites were found in 9 proteins (TpiA, InfA, GlnA and Tkt and RpmE2 in Table S6; Tuf, Ndk, SucC and Eno in Table S7). Phosphorylation sites were found not only in the up and down-regulated proteins (Table S6) but also in proteins without

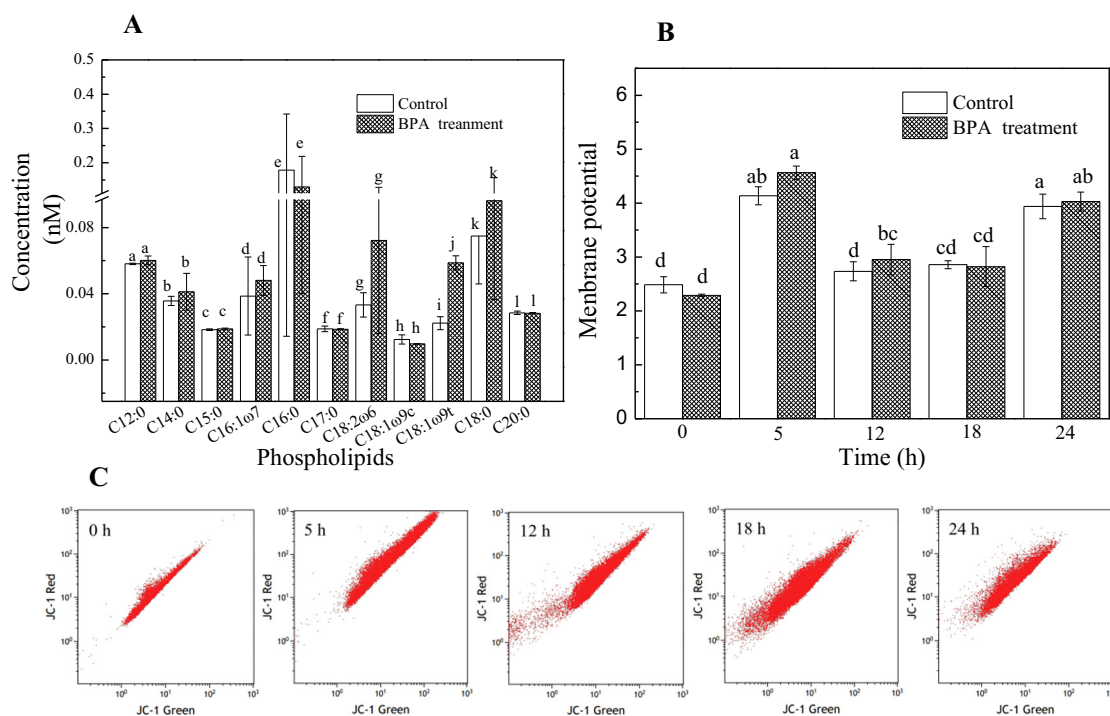
differential expression (Table S8), which inferred that phosphorylation was not a representative posttranslational modification to reflect the influence of BPA on its target proteins.

Table S6 shows that these phosphorylation sites were mainly concentrated on serine, threonine, tyrosine, followed by aspartic acid and arginine. Triosephosphate isomerase (tpiA, upregulation) is a glycolytic enzyme involved in fructose, mannose and inositol phosphate metabolism. Its serine phosphorylation site is on S213 (Macek et al., 2007). Other detected glycolytic enzymes, including glucose-6-phosphate isomerase (Pgi), pyruvate dehydrogenase E1 component subunit alpha (PdhA), pyruvate dehydrogenase E1 component subunit beta (PdhB), and succinyl-CoA ligase [ADP-forming] subunit beta (SucC), were phosphorylated on arginine in stressed environments (Schmidt et al., 2014), whereas their fold-change was not remarkable in the current results.

Phosphotyrosine modification is one significant regulative mechanism which can modulate transcription, translation and elongation (Macek et al., 2007) in eukaryotes and prokaryotes. RpoA (down-regulation), RpoB (no obvious difference) and RpoC (none detected) are related to transcription, which potentially demonstrates that rpoA is easily phosphorylated in different subunits. Tyrosine-phosphorylated protein InfA was upregulated, and its phosphorylation motif is Y (tyrosine) 60 in *Bacillus subtilis* (Jers et al., 2010), which can bind nucleic acids and promote the two subunits IF-2 and IF-3. In addition, the upregulated GlnA could be phosphorylated on tyrosine 180, 327, 398 and 467, respectively. The enzyme activity is influenced by tyrosine phosphorylation (Jers et al., 2010). Therefore, tyrosine phosphorylation plays a certain complicated role in the bacterial cellular process.

### 3.6. Characteristic PLFAs and MP analysis

PLFAs were used as characteristic biomarkers to illustrate the cellular response to stresses (Alvarez-Ordóñez et al., 2009). In this study, seven



**Fig. 6.** (A) The PLFAs concentrations of *B. thuringiensis* before and after bisphenol A treatment. (B) The membrane potential of both the control and bisphenol A treatment groups. (C) The results of bisphenol A treatment with JC-1 Red and JC-1 Green after 0, 5, 12, 18, and 24 h, respectively.

saturated PLFAs, two monounsaturated PLFAs and a polyunsaturated PLFA were detected (Fig. 6A). C16:0 was the most abundant PLFA in both the control and degradation samples, followed by C14:0. Except for C14:0 (1.2 times), C16:1ω7 (1.2 times), C18:2ω6 (2.2 times), C18:1ω9t (2.6 times,  $p$ -value = 0.012) and C18:0 (1.3 times), other PLFAs were not differently expressed. The ratio (0.28) of total unsaturated to total saturated PLFAs of the degradation samples was higher than that (0.23) of the control. Additionally, the ratio of *trans* to *cis*-PLFAs (C18:1ω9t/C18:1ω9c) of the degradation sample was 6.1, whereas that of the control was 1.8. Changes in the proportion of PLFAs affect the membrane fluidity and further influence cellular function. The proportion of PLFAs expressed in *Bacillus* species could be modified under environmental stresses (Diomande et al., 2015). Fig. 6A shows that most PLFAs exhibited an increasing trend after BPA degradation. This suggested a decrease in the fluidity of the cellular membrane because long-chain PLFAs could stabilize the lipid bilayer (Aroui et al., 2016).

C18:2ω6 is a member of the ω-6 fatty acids family which is abundant in the cell membrane (Rodrigues et al., 2016). Its level in the degradation sample was slightly increased compared with the control. C20:4ω6 stemming from C18:2ω6 was not found in the current results. Desaturation of PLFAs is a mechanism for organisms to adapt to environmental change. Generally, C16:0, C16:1ω7 and C18:1ω9 are precursors converted to other PLFAs in bacteria. In the current study, the concentrations of C16:1ω7 and C18:1ω9 (C18:1ω9t) after BPA degradation were obviously higher than those in the control (Fig. 6A), whereas C18:1ω9c was slightly depressed by BPA.

The increasing ratio of unsaturated versus saturated PLFAs could regulate the fluidity of the cellular membrane (Paulucci et al., 2011). Therefore, the *trans/cis* ratio and the conversion rate of *cis*- to *trans*-unsaturated PLFAs could be used as additional representatives of membrane activity (Piotrowska et al., 2016). They have been used as biomarkers to reflect pollutant concentrations (Piotrowska et al., 2017) and environmental stresses (Fischer et al., 2010b; Yao et al., 2014). The significantly increased *trans/cis* ratios ( $p$ -value < 0.01) (C18:1ω9t/C18:1ω9c) of the samples after BPA degradation (Fig. 6A) suggested that BPA induced isomerization of the *cis* to *trans* unsaturated

PLFAs and promoted an increase in the *trans/cis* ratio of unsaturated PLFAs.

Except for these PLFAs results, other direct evidence that glycerol was up-metabolized (Fig. 1) and aldehyde dehydrogenase (*ywdH*) and octanoyltransferase (*lipB/estB*) was related to PLFAs metabolism was also found. *YwdH* is involved in glycolysis/gluconeogenesis, PLFAs metabolism and degradation. Its upregulation suggested the enhancement of PLFAs metabolism. *LipB* is associated with lipoic acid metabolism, catalyzing the transfer of octanoic acid from the octanoyl-acyl carrier protein to the lipoyl domains of lipoate-dependent enzymes. Its overexpression indicated that the cell viability was stimulated, which was consistent with the result of carbon nutrient metabolism (Fig. 1A, B) before and after BPA degradation.

The membrane potential (MP) is the difference in electric potential between the inside and outside of the cell membrane. It is a parameter reflecting membrane permeability. Although Fig. 6B shows no obvious difference after BPA degradation ( $p$ -value > 0.05), MP was significantly different with time extension ( $p$ -value < 0.05) in both the treatment and control samples (Fig. 6C). The MP increased to the maximum value at 5 h because the cells were inoculated from the culture medium to the treatment medium. High concentrations of cations in the degradation medium triggered their transport, resulting in the high MP. After a stable resting stage (12th to 18th hours) with depolarization (MP was decreased), the MP increased again under the stress of starvation over time, which was consistent with the result of the enhanced MP in repopulating cancer cells under starvation (Lee et al., 2016). Alteration of the MP significantly influenced cell metabolism (Wang et al., 2017), along with the variation of PLFAs and differentially expressed proteins in the current study. The difference in the MP further indicated that BPA promoted cell viability and served as a nutrient for *B. thuringiensis* growth and metabolism.

#### 4. Conclusions

*B. thuringiensis* could effectively degrade BPA and its intermediate. The upregulated *BdbD* and down-regulated *SasP-1* played important

roles in maintaining cellular homeostasis. SasP-1 was a potential biomarker to reflect the impairment of spore DNA triggered by BPA. Moreover, BPA increased PLFA synthesis. The significantly increased *trans/cis* ratio ( $p$ -value < 0.01) of C18:1 $\omega$ 9t/C18:1 $\omega$ 9c confirmed that it could be a representative of membrane activity and the cellular response to BPA stress. These findings presented novel insights to the interaction between BPA transformation and cellular metabolism at the pathway and network levels.

## Acknowledgments

The authors would like to thank the National Natural Science Foundation of China (No. 21577049), the Science and Technology Project of Guangdong Province (Nos. 2016B02024007, 2016A020221015), the Science and Technology Project of Guangzhou City (No. 201707010255) and Fundamental research funds for the central universities (No. 21617453) for their financial support.

## Appendix A. Supplementary data

Supplementary data to this article can be found online at <https://doi.org/10.1016/j.scitotenv.2018.05.352>.

## References

- Alvarez-Ordóñez, A., Fernández, A., López, M., Bernardo, A., 2009. Relationship between membrane fatty acid composition and heat resistance of acid and cold stressed *Salmonella senftenberg* CECT 4384. *Food Microbiol.* 26, 347–353.
- Arisawa, K., Mitsudome, H., Yoshida, K., Sugimoto, S., Ishikawa, T., Fujiwara, Y., et al., 2016. Saturated fatty acid in the phospholipid monolayer contributes to the formation of large lipid droplets. *Biochem. Biophys. Res. Commun.* 480, 641–647.
- Arouri, A., Lauritsen, K.E., Nielsen, H.L., Mouritsen, O.G., 2016. Effect of fatty acids on the permeability barrier of model and biological membranes. *Chem. Phys. Lipids* 200, 139–146.
- Basturea, G.N., Zundel, M.A., Deutscher, M.P., 2011. Degradation of ribosomal RNA during starvation: comparison to quality control during steady-state growth and a role for RNase PH. *RNA* 17, 338–345.
- Berger, A., Ziv-Gal, A., Cudiamat, J., Wang, W., Zhou, C., Flaws, J.A., 2016. The effects of in utero bisphenol A exposure on the ovaries in multiple generations of mice. *Reprod. Toxicol.* 60, 39–52.
- Betancourt, A., Mobley, J.A., Wang, J., Jenkins, S., Chen, D.Q., Kojima, K., et al., 2014. Alterations in the rat serum proteome induced by prepubertal exposure to bisphenol A and genistein. *J. Proteome Res.* 13, 1502–1514.
- Brar, S.K., Verma, M., Tyagi, R.D., Valero, J.R., Surampalli, R.Y., 2009. Concurrent degradation of dimethyl phthalate (DMP) during production of *Bacillus thuringiensis* based biopesticides. *J. Hazard. Mater.* 171, 1016–1023.
- Bravo, A., Pacheco, S., Gómez, I., García-Gómez, B., Onofre, J., Soberón, M., 2017. Insecticidal proteins from *Bacillus thuringiensis* and their mechanism of action. In: Fiuza, L.M., Polanczyk, R.A., Crickmore, N. (Eds.), *Bacillus thuringiensis* and *Lysinibacillus sphaericus*: Characterization and Use in the Field of Biocontrol. Springer International Publishing, Cham, pp. 53–66.
- Cho, H., Kim, S.J., Park, H.-W., Oh, M.-J., Yu, S.Y., Lee, S.Y., et al., 2010. A relationship between miRNA and gene expression in the mouse Sertoli cell line after exposure to bisphenol A. *BioChip J.* 4, 75–81.
- Choi, S.Y., Chang, J., Jiang, B., Seol, G.H., Min, S.S., Han, J.S., et al., 2005. Multiple receptors coupled to phospholipase C gate long-term depression in visual cortex. *J. Neurosci.* 25, 11433–11443.
- Collado, N., Buttiglieri, G., Kolvenbach, B.A., Comas, J., Corvini, P.F.X., Rodriguez-Roda, I., 2013. Exploring the potential of applying proteomics for tracking bisphenol A and nonylphenol degradation in activated sludge. *Chemosphere* 90, 2309–2314.
- Crow, A., Lewin, A., Hecht, O., Carlsson Moller, M., Moore, G.R., Hederstedt, L., et al., 2009. Crystal structure and biophysical properties of *Bacillus subtilis* BdbD. An oxidizing thiol:disulfide oxidoreductase containing a novel metal site. *J. Biol. Chem.* 284, 23719–23733.
- Diomande, S.E., Nguyen-The, C., Guinebreiere, M.H., Broussolle, V., Brillard, J., 2015. Role of fatty acids in *Bacillus* environmental adaptation. *Front. Microbiol.* 6, 1–20.
- Domingues, S., Moreira, R.N., Andrade, J.M., dos Santos, R.F., Barria, C., Viegas, S.C., et al., 2015. The role of RNase R in trans-translation and ribosomal quality control. *Biochimie* 114, 113–118.
- Dong, X., Zhang, Z., Meng, S., Pan, C.Y., Yang, M., Wu, X., et al., 2018. Parental exposure to bisphenol A and its analogs influences zebrafish offspring immunity. *Sci. Total Environ.* 610, 291–297.
- Erlendsson, L.S., Hederstedt, L., 2002. Mutations in the thiol-disulfide oxidoreductases BdbC and BdbD can suppress cytochrome c deficiency of CcdA-defective *Bacillus subtilis* cells. *J. Bacteriol.* 184, 1423–1429.
- Esfahani, S.S., Emthiaz, G., Shafiei, R., Ghorbani, N., Esfahani, S.H.Z., 2016. Tolerance induction of temperature and starvation with tricalcium phosphate on preservation and sporulation in *Bacillus amyloliquefaciens* detected by flow cytometry. *Curr. Microbiol.* 73, 366–373.
- Feng, X., Coulombe, P.A., 2015. A role for disulfide bonding in keratin intermediate filament organization and dynamics in skin keratinocytes. *J. Cell Biol.* 209, 59–72.
- Fic, A., Mlakar, S.J., Juvan, P., Mlakar, V., Marc, J., Dolenc, M.S., et al., 2015. Genome-wide gene expression profiling of low-dose, long-term exposure of human osteosarcoma cells to bisphenol A and its analogs bisphenols AF and S. *Toxicol. in Vitro* 29, 1060–1069.
- Fischer, J., Kappelmeyer, U., Kastner, M., Schauer, F., Heipieper, H.J., 2010a. The degradation of bisphenol A by the newly isolated bacterium *Cupriavidus basilensis* JF1 can be enhanced by biostimulation with phenol. *Int. Biodeterior. Biodegrad.* 64, 324–330.
- Fischer, J., Schauer, F., Heipieper, H.J., 2010b. The *trans/cis* ratio of unsaturated fatty acids is not applicable as biomarker for environmental stress in case of long-term contaminated habitats. *Appl. Microbiol. Biotechnol.* 87, 365–371.
- Flint, S., Markle, T., Thompson, S., Wallace, E., 2012. Bisphenol A exposure, effects, and policy: a wildlife perspective. *J. Environ. Manag.* 104, 19–34.
- Haighton, L.A., Hlywka, J.J., Doull, J., Kroes, R., Lynch, B.S., Munro, I.C., 2002. An evaluation of the possible carcinogenicity of bisphenol A to humans. *Regul. Toxicol. Pharmacol.* 35, 238–254.
- Jers, C., Pedersen, M.M., Paspaliari, D.K., Schutz, W., Johnsson, C., Soufi, B., et al., 2010. *Bacillus subtilis* BY-kinase PtkA controls enzyme activity and localization of its protein substrates. *Mol. Microbiol.* 77, 287–299.
- Lee, D.G., Choi, B.K., Kim, Y.H., Oh, H.S., Park, S.H., Bae, Y.S., et al., 2016. The repopulating cancer cells in melanoma are characterized by increased mitochondrial membrane potential. *Cancer Lett.* 382, 186–194.
- Liang, W.X., Deutscher, M.P., 2012. Transfer-messenger RNA-SmpB protein regulates ribonuclease R turnover by promoting binding of HslUV and Lon proteases. *J. Biol. Chem.* 287, 33472–33479.
- Liang, W.X., Deutscher, M.P., 2013. Ribosomes regulate the stability and action of the exoribonuclease RNase R. *J. Biol. Chem.* 288, 34791–34798.
- Lu, A., Peng, Q., Ling, E., 2014. Formation of disulfide bonds in insect prophenoloxidase enhances immunity through improving enzyme activity and stability. *Dev. Comp. Immunol.* 44, 351–358.
- Macek, B., Mijakovic, I., Olsen, J.V., Gnad, F., Kumar, C., Jensen, P.R., et al., 2007. The serine/threonine/tyrosine phosphoproteome of the model bacterium *Bacillus subtilis*. *Mol. Cell. Proteomics* 6, 697–707.
- Maffini, M.V., Rubin, B.S., Sonnenschein, C., Soto, A.M., 2006. Endocrine disruptors and reproductive health: the case of bisphenol-A. *Mol. Cell. Endocrinol.* 254–255, 179–186.
- Mandal, K., Singh, B., Jariyal, M., Gupta, V.K., 2013. Microbial degradation of fipronil by *Bacillus thuringiensis*. *Ecotoxicol. Environ. Saf.* 93, 87–92.
- Moreira, R.N., Domingues, S., Viegas, S.C., Amblar, M., Arraiano, C.M., 2012. Synergies between RNA degradation and trans-translation in *Streptococcus pneumoniae*: cross regulation and co-transcription of RNase R and SmpB. *BMC Microbiol.* 12, 268.
- Pan, Z., Wang, B., Zhang, Y., Wang, Y., Ullah, S., Jian, R., et al., 2015. dbPSP: a curated database for protein phosphorylation sites in prokaryotes. *Database (Oxford)* 2015, 1–8.
- Paulucci, N.S., Medeot, D.B., Dardanelli, M.S., de Lema, M.G., 2011. Growth temperature and salinity impact fatty acid composition and degree of unsaturation in peanut-nodulating rhizobia. *Lipids* 46, 435–441.
- Penniston, J.T., Padanyi, R., Paszty, K., Varga, K., Hegedus, L., Enyedi, A., 2014. Apart from its known function, the plasma membrane Ca<sup>2+</sup> ATPase can regulate Ca<sup>2+</sup> signaling by controlling phosphatidylinositol 4,5-bisphosphate levels. *J. Cell Sci.* 127, 72–84.
- Piotrowska, A., Syguda, A., Chrzanowski, L., Heipieper, H.J., 2016. Toxicity of synthetic herbicides containing 2,4-D and MCPA moieties towards *Pseudomonas putida* mt-2 and its response at the level of membrane fatty acid composition. *Chemosphere* 144, 107–112.
- Piotrowska, A., Syguda, A., Wyrwas, B., Chrzanowski, L., Heipieper, H.J., 2017. Toxicity evaluation of selected ammonium-based ionic liquid forms with MCPP and dicamba moieties on *Pseudomonas putida*. *Chemosphere* 167, 114–119.
- Ramesh, A., Peleh, V., Martinez-Caballero, S., Wollweber, F., Sommer, F., van der Laan, M., et al., 2016. A disulfide bond in the TIM23 complex is crucial for voltage gating and mitochondrial protein import. *J. Cell Biol.* 214, 417–431.
- Rodrigues, H.G., Sato, F.T., Curi, R., Vinolo, M.A.R., 2016. Fatty acids as modulators of neutrophil recruitment, function and survival. *Eur. J. Pharmacol.* 785, 50–58.
- Sasaki, M., Maki, J., Oshiman, K., Matsumura, Y., Tsuchido, T., 2005. Biodegradation of bisphenol A by cells and cell lysate from *Sphingomonas* sp strain AO1. *Biodegradation* 16, 449–459.
- Schmidt, A., Trentini, D.B., Spiess, S., Fuhrmann, J., Ammerer, G., Mechtler, K., et al., 2014. Quantitative phosphoproteomics reveals the role of protein arginine phosphorylation in the bacterial stress response. *Mol. Cell. Proteomics* 13, 537–550.
- Setlow, B., Atluri, S., Kitchel, R., Koziol-Dube, K., Setlow, P., 2006. Role of dipicolinic acid in resistance and stability of spores of *Bacillus subtilis* with or without DNA-protective alpha/beta-type small acid-soluble proteins. *J. Bacteriol.* 188, 3740–3747.
- Tang, L., Wang, L., Ou, H., Li, Q., Ye, J., Yin, H., 2016. Correlation among phenyltins molecular properties, degradation and cellular influences on *Bacillus thuringiensis* in the presence of biosurfactant. *Biochem. Eng. J.* 105, 71–79.
- Tocheva, E.I., Ortega, D.R., Jensen, G.J., 2016. Sporulation, bacterial cell envelopes and the origin of life. *Nat. Rev. Microbiol.* 14, 535–542.
- Wang, L.L., Yi, W.Y., Ye, J.S., Qin, H.M., Long, Y., Yang, M., et al., 2017. Interactions among triphenyltin degradation, phospholipid synthesis and membrane characteristics of *Bacillus thuringiensis* in the presence of D-malic acid. *Chemosphere* 169, 403–412.
- Williams, K.E., Lemieux, G.A., Hassis, M.E., Olshen, A.B., Fisher, S.J., Werb, Z., 2016. Quantitative proteomic analyses of mammary organoids reveals distinct signatures after exposure to environmental chemicals. *PNAS* 113, E1343–E1351.
- Wu, J., Huang, D., Su, X., Yan, H., Sun, Z., 2015. Oral administration of low-dose bisphenol A promotes proliferation of ventral prostate and upregulates prostaglandin D2 synthase expression in adult rats. *Toxicol. Ind. Health* 32, 1848–1858.

- Yang, M., Lee, H.S., Pyo, M.Y., 2008. Proteomic biomarkers for prenatal bisphenol A - exposure in mouse immune organs. *Environ. Mol. Mutagen.* 49, 368–373.
- Yao, H., Chapman, S.J., Thornton, B., Paterson, E., 2014.  $^{13}\text{C}$  PLFAs: a key to open the soil microbial black box? *Plant Soil* 392, 3–15.
- Yin, D., Hu, S., Gu, Y., Wei, L., Liu, S., Zhang, A., 2007. Immunotoxicity of bisphenol A to *Carassius auratus* lymphocytes and macrophages following in vitro exposure. *J. Environ. Sci.* 19, 232–237.
- Zhou, J., Cai, Z., Xing, K., 2011. Potential mechanisms of phthalate ester embryotoxicity in the abalone *Haliotis diversicolor supertexta*. *Environ. Pollut.* 159, 1114–1122.
- Zhou, N.A., Kjeldal, H., Gough, H.L., Nielsen, J.L., 2015. Identification of putative genes involved in bisphenol a degradation using differential protein abundance analysis of *Sphingobium* sp BiD32. *Environ. Sci. Technol.* 49, 12232–12241.